

This paper is published in:

S.A. Krasnikov, S. Murphy, N. Berdunov, A.P. McCoy, K. Radican, and I.V. Shvets, *Self-limited growth of triangular PtO₂ nanoclusters on the Pt(111) surface*. *Nanotechnology* **21** (2010) 335301.

Self-limited growth of triangular PtO₂ nanoclusters on the Pt(111) surface

S. A. Krasnikov¹, S. Murphy², N. Berdunov, A. P. McCoy, K. Radican and I. V. Shvets

Centre for Research on Adaptive Nanostructures and Nanodevices (CRANN), School of Physics, Trinity College Dublin, Dublin 2, Ireland.

Abstract

The high temperature oxidation of the Pt(111) surface by molecular oxygen has been studied using scanning tunnelling microscopy (STM) and low-energy electron diffraction (LEED). Results indicate a self-limited growth of well-ordered PtO₂ nanoclusters which have an O-Pt-O trilayer structure. Each nanocluster has a triangular shape and nucleates at the Pt(111) surface step edge due to mobility of Pt atoms. The triangular PtO₂ nanoislands on the upper and lower Pt(111) terraces represent two mirror domains with the mirror plane perpendicular to the substrate and aligned along the [1-10] direction of the latter. LEED data obtained from the nanostructured PtO₂/Pt(111) surface show a characteristic (2×2) pattern. Different oxidation conditions lead to the formation of chemisorbed oxygen on the Pt(111) surface alongside PtO₂ nanoclusters. Oxygen adsorbs on the surface forming variety of structures which result in (3×3), (5×5) and (7×7) LEED patterns.

1. Introduction

Interaction of oxygen with the Pt(111) surface has been studied intensively during last decade, largely due to the significance of platinum for many industrial applications of heterogeneous catalysis, especially as a catalyst for oxidation reactions [1, 2], a principal example of which is CO oxidation to CO₂ in automotive catalytic converters [3]. Oxidation of Pt can result in a variety of oxygen phases on the surface ranging from a dilute chemisorbed layer to a bulk oxide. Formation of two-dimensional surface oxide is of particular interest since it can lead to the nucleation of three-dimensional oxide particles [4, 5]. Platinum oxides play a crucial role in a number of chemical reactions [6, 7]. Among them is PtO₂, which is a well-known hydrogenation catalyst. Recent studies show that the oxides formed on Pt surfaces are the most efficient for the oxidation of CO compared to the chemisorbed oxygen [2, 8-11]. Furthermore, small oxide clusters, which always exhibit structural defects at edges and corners, are more reactive than single crystals covered by a complete layer of a surface oxide [11-13]. The ability to control the formation, size and spatial separation of oxide nanoparticles is important for improvement of their catalytic activity and effectiveness. This constitutes a major driving force in exploring nanotechnology in catalysis [14].

Oxygen adsorbs molecularly on the Pt(111) substrate below 160 K [15] but dissociates on the surface at higher temperatures forming a p(2×2) adlayer structure with oxygen atoms occupying fcc hollow sites [16]. The surface saturates at a coverage of 0.25 monolayer (ML) due to strong lateral repulsive interactions between the oxygen atoms [17]. Higher oxygen coverages or oxide overlayers can be obtained either by annealing in O₂ [18] or by utilizing NO₂ [19, 20], ozone [21] or atomic oxygen [4, 22]. It was found that oxygen occupies

¹ Author to whom any correspondence should be addressed. E-mail: krasniks@tcd.ie

² Present address: Center for Individual Nanoparticle Functionality (CINF), Technical University of Denmark, 2800 Kongens Lyngby, Denmark.

different surface sites (fcc and hcp hollow sites) at intermediate coverages in the range of 0.25-0.7 ML [20].

Using temperature programmed desorption (TPD) a minimum in the activation energy for oxygen desorption was observed at a coverage of around 1 ML, indicating that at this coverage there is a phase change from chemisorbed oxygen to a surface oxide [21]. Further confirmation of surface oxide formation at this coverage was provided by an angle-resolved X-ray photoelectron spectroscopy (XPS) study of the Pt(111) surface exposed to atomic oxygen at 300 K [22]. XPS confirmed the presence of an oxide in the upper two layers of the surface, which displayed a streaked (1×1) LEED pattern. A recent study of Pt(111) oxidation at 450 K using atomic oxygen shows formation of a chemisorbed oxygen layer up to a coverage of 0.75 ML, after which particles of platinum oxide develop on the surface [4]. A sharp p(2×2) LEED pattern was observed for coverages up to 0.25 ML, corresponding to oxygen adsorption in fcc hollow sites, while a (2×2) LEED pattern corresponding to a higher density structure involving both fcc and hcp sites persisted up to 0.5 ML [4]. For higher coverages the oxidized Pt(111) surface shows a (1×1) LEED pattern until it disappears at 1.1 ML, indicating that the nucleation of a surface oxide layer greatly disrupts the surface order.

In the present work we use scanning tunnelling microscopy and low-energy electron diffraction to study oxide structures on the Pt(111) surface formed by high temperature annealing at 1000-1300 K and cooling in a partial oxygen pressure in the range of $5-10 \times 10^{-5}$ mbar. While there have been STM studies of oxygen structures on Pt(111) at low coverages [23–25], it appears that no attempt has been made so far to use STM for the study of the structures produced at higher coverage, including nucleation of oxide overlayers. The results of this work yield important information on the structure and formation of the PtO₂ nanoclusters grown on the Pt(111) surface which can be utilised as ordered and uniformly sized catalytic centres. Furthermore, these results show that a simple preparation procedure can lead to a formation of well-ordered PtO₂ nanoclusters.

2. Experimental details

All experiments were performed in an ultra-high-vacuum (UHV) system equipped with a home-built room-temperature STM, LEED and Auger electron spectroscopy (AES) consisting of an analysis chamber (with a base pressure of 2×10^{-10} mbar) and a preparation chamber (8×10^{-10} mbar). An electrochemically etched polycrystalline tungsten tip was used to record STM images in constant current mode. The voltage V corresponds to the sample bias with respect to the tip. No drift corrections have been applied to any of the STM images presented in this paper. A single-crystal Pt(111) surface (Surface Preparation Laboratory) was used as a substrate. The Pt(111) crystal was cleaned *in situ* by repeated cycles of annealing at 950 K in oxygen atmosphere of 10^{-6} mbar followed by a short (5 min) anneal at 1200-1300 K in UHV until a LEED pattern with sharp diffraction spots was obtained. The sample temperature was monitored using an infra-red pyrometer (Ircan, Ultimex UX-20P).

The Pt(111) surface was oxidised by annealing at 1000-1350 K in an oxygen partial pressure in the range of 10^{-6} to 10^{-5} mbar for 5-30 min, followed by cooling down to room temperature in oxygen atmosphere. It should be noted that the anneal temperatures used in this work were much higher than the decomposition temperature (approximately 800 K) of surface oxide on the Pt(111) [21, 22]. The oxide structures in this study were formed as the surface was cooling down. The estimated cooling rate was approximately 20 K per sec in the first 10 sec of cooling dropping to 10 K per sec after 20 sec.

3. Results and discussion

After 30 min exposure of the clean Pt(111) surface at room temperature to oxygen atmosphere with a partial pressure of 1×10^{-6} mbar, oxygen is chemisorbed on the surface

leading to a sharp (2×2) LEED pattern. A surface oxide structure corresponding to a (2×2) LEED pattern was also obtained by annealing the Pt(111) in oxygen partial pressure of 5×10^{-5} mbar at substrate temperatures between 1250 K and 1350 K for 5-30 min followed by cooling down to room temperature in O₂. LEED patterns taken from the clean and oxidized Pt (111) surface are shown in Figure 1. Slight variations in the preparation conditions lead to the same sharp (2×2) LEED pattern suggesting the stability of the oxide structure formed on the surface during high temperature oxidation. This structure is attributed to the formation of the (0001)-oriented α -PtO₂ which is the most stable Pt oxide phase observed on the Pt(111) surface [1, 18, 26-28]. It is well known that a surface oxide does not coexist with the pure metal but rather with a significant concentration of adsorbed oxygen on metal surfaces [12]. Under such preparation conditions, which involve cooling down the surface to room temperature in oxygen atmosphere of 5×10^{-5} mbar, oxygen is most likely chemisorbed on the fcc hollow sites of the surface alongside the formation of the α -PtO₂. The chemisorbed oxygen occupying these surface sites also contributes to the (2×2) LEED pattern.

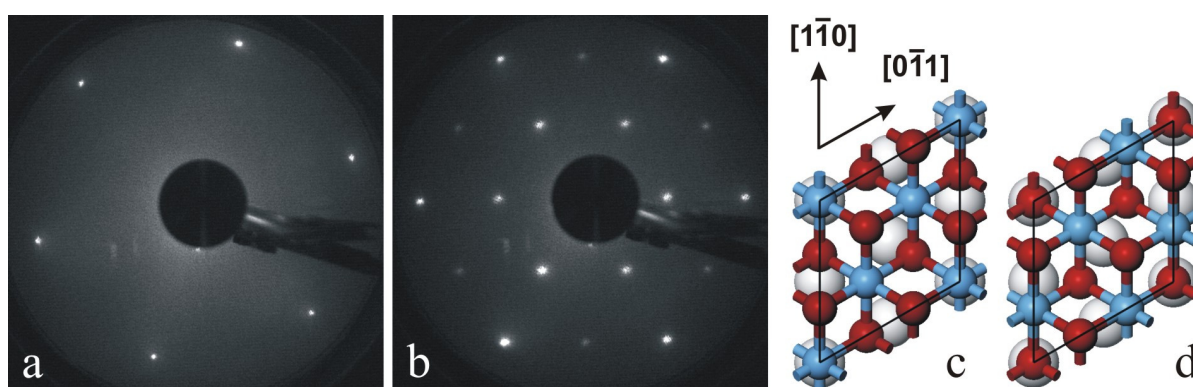


Figure 1. (a) (1×1) LEED pattern of the clean Pt(111) surface and (b) (2×2) pattern obtained by annealing the Pt(111) surface at 1300 K for 5 min in an oxygen partial pressure of 5×10^{-5} mbar, followed by cooling down to room temperature at this oxygen pressure. Both patterns were obtained with a primary electron beam energy of 62 eV. (c) and (d) Schematic models of two possible structures for the α -PtO₂ (0001) (2×2) overlayer on the Pt(111). Pt atoms in the oxide (blue spheres) occupy on-top positions over every second Pt atom in the surface (large light grey spheres) (c) and O atoms in the oxide (red spheres) occupy on-top positions over Pt atoms in the surface (d).

Two models for the α -PtO₂ structure with different registries between the oxide overlayer and the surface are shown in Figures 1c and 1d. In the first case some Pt atoms in the oxide occupy on-top positions over Pt atoms in the surface (Figure 1c), while in the second case some O atoms in the oxide occupy on-top positions over Pt atoms in the surface (Figure 1d). In both models the α -PtO₂ (0001) layer is rotated by 30° with respect to the Pt(111) surface to minimise the lattice mismatch. The lattice parameters of Pt(111) and α -PtO₂ (0001) are 0.278 nm and 0.312 nm respectively. To form a (1×1) epitaxial overlayer on the Pt(111) surface, the α -PtO₂ (0001) layer needs to accommodate a compressive strain of roughly 11%. In turn, by forming a coincidence lattice between a $(\sqrt{3} \times \sqrt{3})R30^\circ$ unit cell of the α -PtO₂ (0001) overlayer and a (2×2) cell of the Pt(111) surface, the strain in the α -PtO₂ (0001) overlayer is significantly reduced to a small tensile strain of approximately 2%.

STM data taken from the oxidized Pt(111) surface show the formation of ordered PtO₂ nanoclusters at the step edges of the substrate. Typical STM images of these nanoclusters are shown in Figure 2. The PtO₂ initially nucleates along the substrate step edges, forming triangular islands that decorate both the upper and lower terraces, as shown in Figure 2a. The apparent height of the islands varies slightly with the tunnelling parameters, but is of the order of 3.2 Å at a tunnelling bias of -0.7 V and 3.5 Å at -1.5 V. The height difference between the islands on the upper and lower terraces is equal to 2.3 ± 0.2 Å, which

corresponds to the height of the Pt(111) substrate step edge (see Figure 2b). This value is in excellent agreement with the theoretically predicted value of 2.33 \AA for the step height of the Pt(111) surface. The island density is strongly correlated to the substrate step density, with a much higher island density present on those regions where the substrate steps are bunched, as shown in Figure 2c. By resolving the atomic corrugation on the surface of the Pt oxide nanoisland (see Figure 2d) it was found that atoms form close packed hexagonal structure with the periodicity of $5.6 \pm 0.2 \text{ \AA}$, which corresponds to the (2×2) structure. The islands are therefore attributed to one of the $\alpha\text{-PtO}_2$ (0001) (2×2) coincidence structures shown schematically in Figures 1c and 1d.

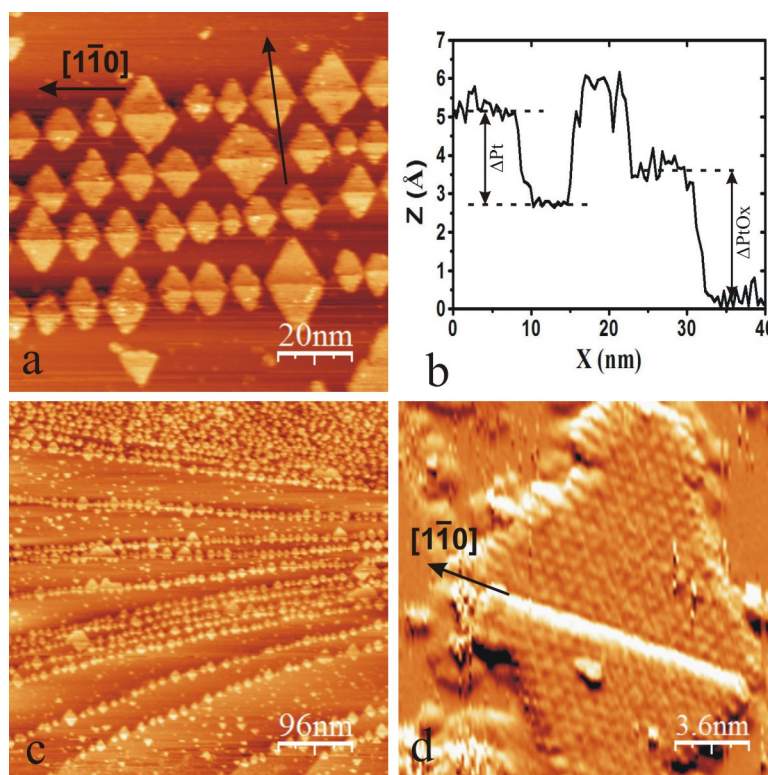


Figure 2. STM images of platinum oxide nanoislands nucleated at the Pt(111) step edges after annealing the surface at 1300 K for 5 min in an oxygen partial pressure of 5×10^{-5} mbar, followed by cooling down to room temperature at this oxygen pressure. (a) Correlated growth of the triangular islands on both the upper and lower substrate terraces, image size = $100 \text{ nm} \times 100 \text{ nm}$, $I = 0.1 \text{ nA}$, $V = -1.5 \text{ V}$. (b) A line profile taken along the direction indicated in (a) by an arrow. The substrate step height is $2.3 \pm 0.2 \text{ \AA}$, while the oxide island height is $3.2 \pm 0.2 \text{ \AA}$. (c) The oxide nanoislands density increases dramatically over step-bunched regions of the surface, image size = $480 \text{ nm} \times 480 \text{ nm}$, $I = 0.1 \text{ nA}$, $V = -1.8 \text{ V}$. (d) The (2×2) Pt oxide structure of the nanoisland, image size = $18 \text{ nm} \times 18 \text{ nm}$, $I = 0.05 \text{ nA}$, $V = -0.7 \text{ V}$.

The formation of ordered uniformly sized PtO_2 nanoclusters on the Pt(111) surface can be attributed to the mobility of Pt atoms at the substrate step edges. To form such oxide nanoclusters the Pt(111) surface was annealed at 1300 K for 5 min in an oxygen partial pressure of 5×10^{-5} mbar, followed by cooling down to room temperature at this oxygen pressure. With such a preparation procedure PtO_2 nanoclusters are formed as the surface cools down. Previous studies have shown that the decomposition temperature of surface oxide on the Pt(111) is approximately 800-850 K [1, 21, 22]. It is believed that the PtO_2 starts to nucleate at substrate step edges when temperature decreases to 850 K during cooling down in oxygen atmosphere. The growth of the PtO_2 nanoislands is promoted by the mobility of Pt atoms at this temperature. The Pt atoms leave the substrate step edge moving on top of the first oxygen layer to form a middle layer in the O-Pt-O trilayer oxide structure. Very few Pt

oxide nanoclusters formed in the middle of the Pt(111) terraces were observed after such a preparation procedure. Furthermore, the island density was much higher in the step-bunched regions of the substrate (see Figure 2c). These findings further confirm the oxide growth model based on mobility of Pt atoms at the substrate step edges. The supply of highly mobile Pt atoms from the Pt(111) substrate step edges leads to a formation of triangular oxide nanoclusters. The growth of the PtO₂ nanoclusters can be described as self-limited. It continues until the entire substrate step edge is covered by the oxide and no mobile Pt atoms are provided anymore. PtO₂ nanoislands grow uniformly on the upper and lower substrate terraces as the surface cools down producing equally sized oxide triangles on both terraces. These almost identical Pt oxide triangles represent mirror images of each other and share the same base side which is aligned along the [1-10] direction of the substrate. The apparent height of the Pt oxide nanoislands, which is measured to be $3.2 \pm 0.2 \text{ \AA}$, suggests a formation of the O-Pt-O trilayer structure on the surface.

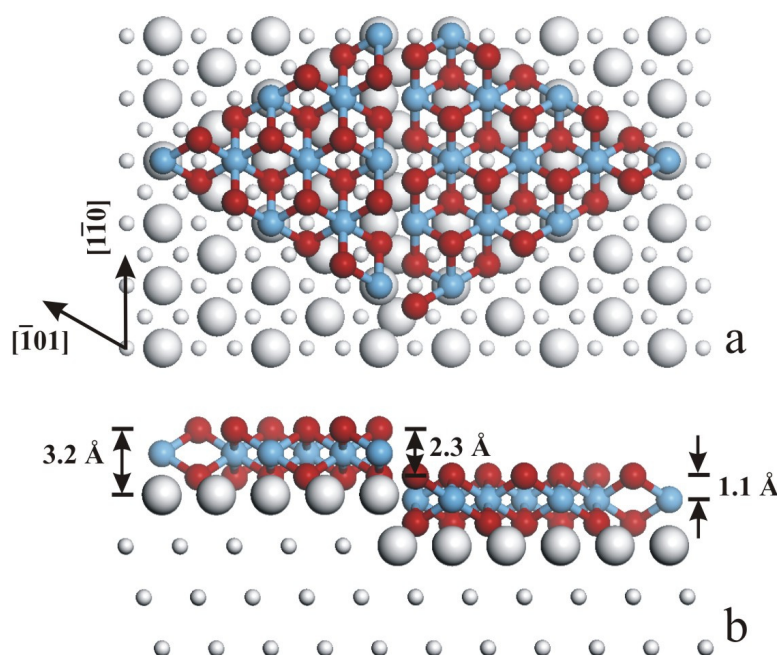


Figure 3. Model for the triangular platinum oxide nanoislands nucleated at the step edge on the upper and lower terraces of the Pt(111) surface: top view (a) and side view (b). The islands are formed by the α -PtO₂ (0001) overlayer which has a (2×2) coincidence structure with the substrate. The Pt atoms in the oxide layer are denoted by blue spheres, the O atoms by red spheres, the Pt atoms of the Pt(111) surface are denoted by large light grey spheres, while the bulk Pt atoms are indicated by small light grey spheres.

The corresponding model of the triangular platinum oxide nanoislands that nucleate at the step edge on the upper and lower terraces of the Pt(111) surface is shown in Figure 3. The islands have the α -PtO₂ (0001) overlayer structure formed by an O-Pt-O trilayer. The triangular nanoislands on the upper and lower terraces represent two mirror domains with the mirror plane perpendicular to the substrate and aligned along the [1-10] direction of the latter. Furthermore, these domains share a continuous oxygen layer formed by the lower oxygen layer of the upper terrace island and the upper oxygen layer of the lower terrace island.

Under extended oxidising conditions at a lower substrate temperature, Pt oxide islands begin to nucleate on the substrate terraces alongside with those formed at the substrate step edges, as shown in Figures 4a and 4b. Here the Pt(111) surface was annealed at 1150 K for 20 min in an oxygen partial pressure of 5×10^{-5} mbar, followed by cooling down to room temperature at this oxygen pressure. PtO₂ nanoislands nucleated at the substrate step edges

have a triangular shape similar to those shown in Figure 2. It is evident from Figure 4a that the Pt oxide islands produce a faceting of the Pt(111) substrate steps when the latter are not aligned along the $[1-10]$ directions favoured for the oxide growth. In this case the substrate step edge has a zig-zag shape after formation of the oxide nanoclusters. Only those regions of the step edge, which are parallel to the $[1-10]$ directions, are covered by the PtO_2 triangular nanoclusters.

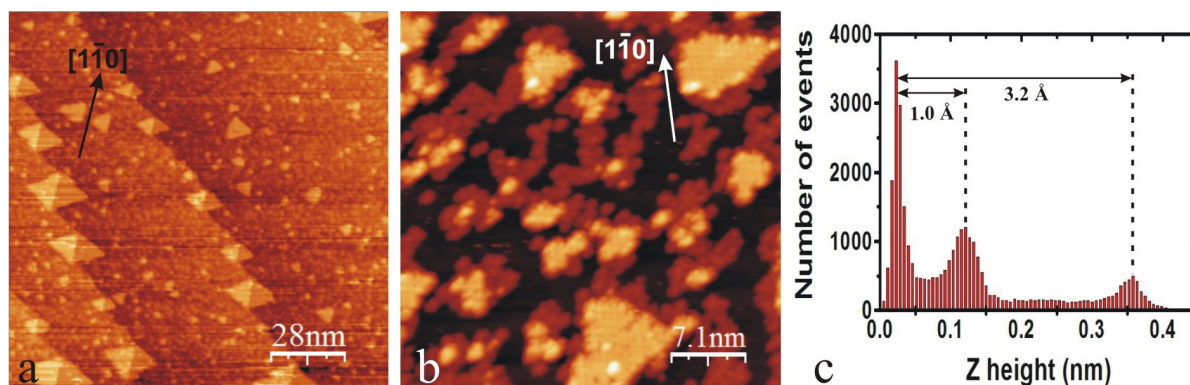


Figure 4. STM images of platinum oxide nanoclusters formed on the Pt(111) after annealing the surface at 1150 K for 20 min in an oxygen partial pressure of 5×10^{-5} mbar, followed by cooling down to room temperature at this oxygen pressure. (a) Image size = 140 nm \times 140 nm, $I = 0.05$ nA, $V = -1.7$ V. (b) Incompleted O-Pt-O trilayer structure of Pt oxide clusters formed in the middle of substrate terrace, image size = 36 nm \times 36 nm, $I = 0.05$ nA, $V = -0.7$ V. (c) The corresponding height histogram from the image b.

Figure 4b shows the presence of an incomplete first oxygen layer on the Pt(111) surface (dark protrusions) alongside the Pt oxide islands (bright protrusions). From the corresponding roughness analysis shown in Figure 4c the apparent height of the first oxygen layer was measured to be 1.0 Å and is therefore attributed to a chemisorbed oxygen layer on the surface. In turn, completed PtO_2 nanoislands have the apparent height of 3.2 Å, which further confirms the O-Pt-O trilayer structure of the oxide clusters. It is obvious that the oxidation at lower substrate temperatures increases the amount of chemisorbed oxygen forming the first adlayer on the Pt(111) terraces. This is due to lower mobility of Pt atoms at such temperatures that leads to a large number of incomplete PtO_2 nanoislands. Some of these nanoclusters formed on the Pt(111) terraces have a triangular shape, but they have no mirror counterparts in contrast to the PtO_2 nanoclusters nucleated at the substrate step edges.

Annealing the Pt(111) surface at 1100 K for 30 min in an oxygen partial pressure of 5×10^{-5} mbar, followed by cooling down to room temperature at this oxygen pressure leads to a formation of a honeycomb Pt oxide structure. The corresponding STM images are shown in Figures 5a and 5b. In this case the oxide overlayer has a high number of defects. The average periodicity of the observed honeycomb Pt oxide structure is 2.0 ± 0.2 nm. The apparent height of this oxide structure is equal to 1.5 ± 0.1 Å, which is half the height of the triangular PtO_2 nanoislands shown in Figures 2 and 4. These disordered Pt oxide islands may represent sub-surface oxide, which has the O-Pt-O trilayer structure. The formation of similar Pt oxide structures on the Pt(111) surface was observed previously by exposing the surface to NO_2 at 450 K [29]. It was found that at oxygen coverages higher than 0.4 ML Pt oxide chains with apparent height of 1.7 Å develop on the surface. At a coverage of 0.75 ML the chains form an interconnected network of Y-shaped structures with regions locally resembling a honeycomb structure [29]. The Pt oxide chain formation was attributed to a buckling of Pt atoms out of the surface by as much as 0.8 Å as a result of coordinating with multiple oxygen atoms [29-31].

The formation of honeycomb Pt oxide structure was also proposed by Parkinson et. al. [22] who have studied the reaction of atomic oxygen with the Pt(111) surface using X-ray photoelectron spectroscopy and co-axial impact collision ion scattering spectroscopy. They have found that exceeding the critical coverage of oxygen on the Pt surface leads to a transition from chemisorbed oxygen to an oxide layer, which in turn results in the formation of sub-surface oxide. This sub-surface oxide structure is formed at high substrate temperatures by substitutional incorporation of O in the second Pt layer along with oxygen adsorption in the surface hollow sites [22]. The Pt sub-surface oxide formation on the Pt(111) surface is further confirmed by the presence of an additional partial layer (marked B in Figures 5a and 5b) about 0.8 Å below the honeycomb structure (marked A) and approximately 0.7 Å above the Pt(111) surface (marked C in Figures 5a and 5b). These height differences were almost identical in STM images acquired at several values of the bias voltage in the range from -2.6 V to +2.6 V. It is believed that this layer represents a Pt surface layer which is lifted up due to substitutional incorporation of O atoms underneath it. Furthermore, density functional theory (DFT) calculations show that the formation of Pt sub-surface oxide on the Pt(111) surface becomes more favoured compared to surface oxide as an oxygen coverage exceeds 0.75 ML [31]. According to DFT the top Pt layer is pushed up from the surface by 0.7-0.8 Å due to incorporation of O atoms [31], which is in excellent agreement with the STM results presented in this work. Above this coverage the Pt oxide chains eventually merge into the Pt oxide honeycomb structure and transform further into quasi two-dimensional α -PtO₂ (0001) film.

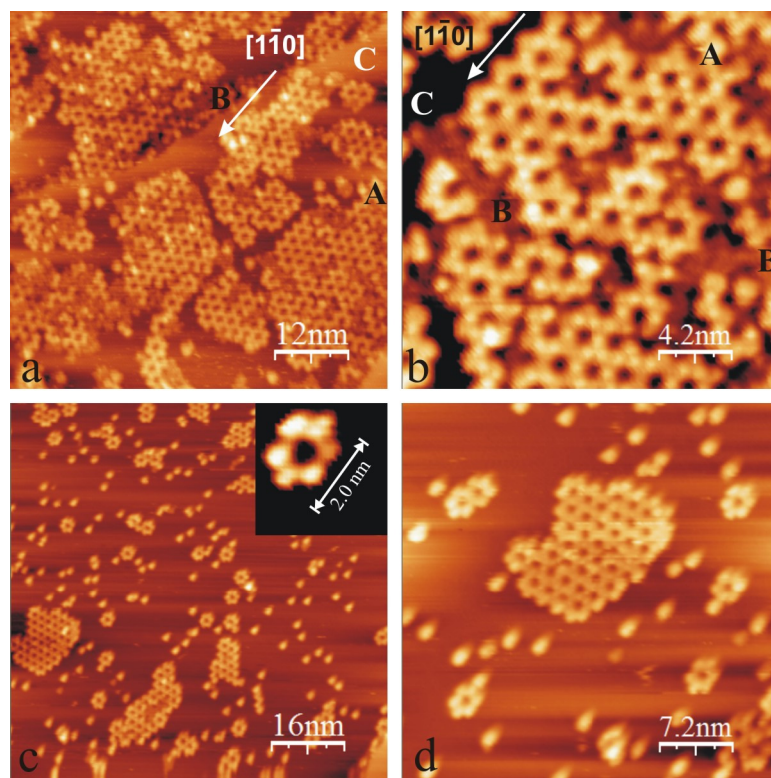


Figure 5. STM images of platinum oxide formed on the Pt(111) after annealing the surface at 1100 K for 30 min in an oxygen partial pressure of 5×10^{-5} mbar, followed by cooling down to room temperature at this oxygen pressure. (a) Image size = 60 nm \times 60 nm, $I = 0.1$ nA, $V = -1.05$ V. (b) Incomplete honeycomb structure of Pt sub-surface oxide, image size = 21 nm \times 21 nm, $I = 0.03$ nA, $V = +0.8$ V. (c) and (d) Oxygen structures formed on the Pt(111) at low surface coverage, image size = 80 nm \times 80 nm, $I = 0.05$ nA, $V = -1.7$ V. (d) Image size = 36 nm \times 36 nm, $I = 0.05$ nA, $V = -1.7$ V.

Annealing the Pt(111) surface at temperatures below 1100 K in oxygen atmosphere of 5×10^{-5} mbar and cooling down in UHV results in a variety of oxygen structures on the surface. These include single oxygen atoms, hexagonal rings (see Figure 5c, inset), double ring structures and fragments of ordered honeycomb structure. The corresponding STM images are shown in Figures 5c and 5d. In this case the total oxygen coverage is significantly lower than the one obtained during cooling the substrate in oxygen atmosphere.

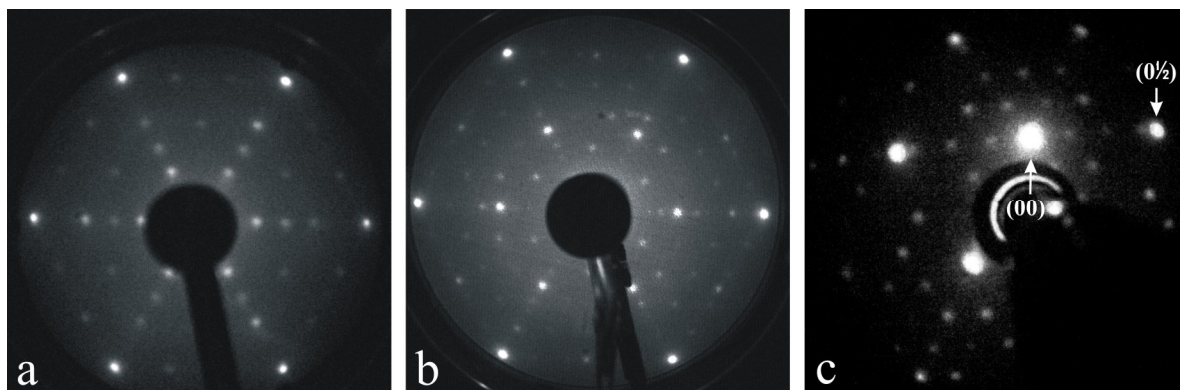


Figure 6. LEED patterns obtained from the oxidized Pt(111) surface prepared at different oxidation conditions. (a) $(2 \times 2) + (3 \times 3)$ LEED pattern taken at 54 eV from the Pt(111) surface after exposure to 5×10^{-5} mbar of O_2 for 5 min at 1125 K. (b) $(2 \times 2) + (5 \times 5)$ LEED pattern taken at 54 eV from the Pt(111) surface after exposure to 5×10^{-5} mbar of O_2 for 30 min at 1300 K. (c) $(2 \times 2) + (7 \times 7)$ LEED pattern taken at 42 eV from the Pt(111) surface after exposure to 5×10^{-5} mbar of O_2 for 30 min at 1100 K. The LEED pattern (c) is positioned off-centre to reveal the specular spot.

Chemisorbed oxygen structures on the Pt(111) surface result in different LEED patterns observed after substrate exposure to molecular oxygen at different temperatures. Examples of (3×3) , (5×5) and (7×7) LEED patterns are shown in Figure 6. The (3×3) LEED pattern is attributed to a chemisorbed oxygen that occupies all-fcc hollow sites on the surface as proposed by DFT [31, 32]. The (7×7) LEED pattern is attributed to a formation of the honeycomb Pt sub-surface oxide structure with a periodicity of 2.0 nm on the Pt(111) surface. It is noted that for almost all of the LEED patterns obtained from the oxidized Pt(111), a (2×2) structure was observed to co-exist on the surface. This (2×2) pattern results from the PtO_2 nanoclusters formed on the surface alongside chemisorbed oxygen as well as from chemisorbed oxygen occupying fcc hollow sites of the substrate. This agrees well with previous results indicating that the (2×2) α - PtO_2 (0001) structure is the most common and stable Pt oxide phase formed on the Pt(111) surface [1, 18, 26-28].

In conclusion, the high temperature oxidation of the Pt(111) surface by molecular oxygen has been investigated using STM and LEED. Annealing the Pt(111) surface at 1250-1350 K for 5-30 min in an oxygen partial pressure of 5×10^{-5} mbar followed by cooling down to room temperature in this oxygen atmosphere results in a self-limited growth of well-ordered PtO_2 nanoclusters which have the O-Pt-O trilayer structure. Under such preparation conditions PtO_2 nanoclusters are formed as the surface cools down. Each nanocluster has a triangular shape and nucleates at the Pt(111) surface step edge due to mobility of Pt atoms. The triangular PtO_2 nanoislands on the upper and lower Pt(111) terraces represent two mirror domains with the mirror plane perpendicular to the substrate and aligned along the $[1-10]$ direction of the latter. LEED data obtained from the nanostructured $PtO_2/Pt(111)$ surface show a characteristic (2×2) pattern. The PtO_2 nanoclusters grown on the Pt(111) surface can be utilised as ordered and uniformly sized catalytic centres. Different oxidation conditions at lower substrate temperatures lead to the formation of chemisorbed oxygen on the Pt(111) surface alongside PtO_2 nanoclusters. Oxygen adsorbs on the surface forming variety of structures which result in (3×3) , (5×5) and (7×7) LEED patterns.

Acknowledgements

This work was supported by Science Foundation Ireland (grant number 00/PI.1/C042).

References

- [1] Seriani N, Pompe W and Ciacchi L C 2006 *J. Phys. Chem. B* **110** 14860
- [2] Hendriksen B L M and Frenken J W M 2002 *Phys. Rev. Lett.* **89** 046101
- [3] McBride J R, Graham G W, Peters C R and Weber W H 1991 *J. Appl. Phys.* **69** 1596
- [4] Weaver J F, Chen J-J and Gerrard A L 2005 *Surf. Sci.* **592** 83
- [5] Shumbera R B, Kan H H and Weaver J F 2007 *Surf. Sci.* **601** 4809
- [6] Park K-T, Novikov D L, Gubanov V A and Freeman A J 1994 *Phys. Rev. B* **49** 4425
- [7] Zhensheng J, Chanjuan X, Qingmei Z, Feng Y, Jiazheng Z and Jinzhen X 2003 *J. Mol. Catal. A* **191** 61
- [8] Ackermann M D, Pedersen T M, Hendriksen B L M, Robach O, Bobaru S C, Popa I, Quiros C, Kim H, Hammer B, Ferrer S and Frenken J W M 2005 *Phys. Rev. Lett.* **95** 255505
- [9] Li W X, Österlund L, Vestergaard E K, Vang R T, Matthiesen J, Pedersen T M, Lægsgaard E, Hammer B and Besenbacher F 2004 *Phys. Rev. Lett.* **93** 146104
- [10] Sun Y-N, Giordano L, Goniakowski J, Lewandowski M, Qin Z-H, Noguera C, Shaikhutdinov S, Pacchioni G and Freund H-J 2010 *Angew. Chem. Int. Ed.* **49** 4418
- [11] Pedersen T M, Li W X and Hammer B 2006 *Phys. Chem. Chem. Phys.* **8** 1566
- [12] Lundgren E, Mikkelsen A, Andersen J N, Kresse G, Schmid M and Varga P 2006 *J. Phys.: Condens. Matter* **18** R481
- [13] Klikovits J, Schmid M, Gustafson J, Mikkelsen A, Resta A, Lundgren E, Andersen J N and Varga P 2006 *J. Phys. Chem. B* **110** 9966
- [14] Zhong C-J, Luo J, Fang B, Wanjala B N, Njoki P N, Loukrakpam R and Yin J 2010 *Nanotechnology* **21** 062001
- [15] Steininger H, Lehwald S and Ibach H 1982 *Surf. Sci.* **123** 1
- [16] Materer N, Starke U, Barbieri A, Döll R, Heinz K, Van Hove M A and Somorjai G A 1995 *Surf. Sci.* **325** 207
- [17] Norton P R, Davies J A and Jackman T E 1982 *Surf. Sci.* **122** L593
- [18] Salmerón M, Brewer L and Somorjai G A 1981 *Surf. Sci.* **112** 207
- [19] Parker D H, Bartram M E and Koel B E 1989 *Surf. Sci.* **217** 489
- [20] Jerdev D I, Kim J, Batzill M and Koel B E 2002 *Surf. Sci.* **498** L91
- [21] Saliba N A, Tsai Y-L, Panja C and Koel B E 1999 *Surf. Sci.* **419** 79
- [22] Parkinson C R, Walker M and McConville C F 2003 *Surf. Sci.* **545** 19
- [23] Feibelman P J, Esch S and Michely T 1996 *Phys. Rev. Lett.* **77** 2257
- [24] Zambelli T, Barth J V, Wintterlin J and Ertl G 1997 *Nature* **390** 495
- [25] Stipe B C, Rezaei M A, Ho W, Gao S, Persson M and Lundqvist B I 1997 *Phys. Rev. Lett.* **78** 4410
- [26] Li W X and Hammer B 2005 *Chem. Phys. Lett.* **409** 1
- [27] Seriani N and Mittendorfer F 2008 *J. Phys.: Condens. Matter* **20** 184023
- [28] Ellinger C, Stierle A, Robinson I K, Nefedov A and Dosch H 2008 *J. Phys.: Condens. Matter* **20** 184013
- [29] Devarajan S P, Hinojosa J A and Weaver J F 2008 *Surf. Sci.* **602** 3116
- [30] Helveg S, Lorensen H T, Horch S, Lægsgaard E, Stensgaard I, Jacobsen K W, Norskov J K and Besenbacher F 1999 *Surf. Sci.* **430** L533
- [31] Hawkins J M, Weaver J F and Asthagiri A 2009 *Phys. Rev. B* **79** 125434
- [32] Getman R B, Xu Y and Schneider W F 2008 *J. Phys. Chem. C* **112** 9559